AIAA JOURNAL
Vol. 31, No. 11, November 1993

Effect of Acoustic Coupling on Random and Harmonic Plate Vibrations

Abdelkader Frendi*
Analytical Services and Material Inc., Hampton, Virginia 23666
and
Jay Robinson†
NASA Langley Research Center, Hampton, Virginia 23681

The effect of acoustic coupling on random and harmonic plate vibrations is studied using two numerical models. In the coupled model, the plate response is obtained by integration of the nonlinear plate equation coupled with the nonlinear Euler equations for the surrounding acoustic fluid. In the uncoupled model, the nonlinear plate equation with an equivalent linear viscous damping term is integrated to obtain the response of the plate subject to the same excitation field. For a low-level, narrow-band excitation, the two models predict the same plate response spectra. As the excitation level is increased, the response power spectrum predicted by the uncoupled model becomes broader and more shifted toward the high frequencies than that obtained by the coupled model. In addition, the difference in response between the coupled and uncoupled models at high frequencies becomes larger. When a high intensity harmonic excitation is used, causing a nonlinear plate response, both models predict the same frequency content of the response. However, the levels of the harmonics and subharmonics are higher for the uncoupled model. Comparisons to earlier experimental and numerical results show that acoustic coupling has a significant effect on the plate response at high excitation levels. Its absence in previous models may explain in part the discrepancy between predicted and measured responses.

I. Introduction

IT is well known in structural dynamics that linear plate theory cannot be used to accurately predict structural responses at high excitation levels. In an attempt to overcome this weakness, several nonlinear plate models have been proposed. The nonlinearities introduced in the various models can be classified in two categories: geometric nonlinearity or material nonlinearity. The nonlinear model based on the geometric nonlinearity, also referred to as the large deflection model, has been extensively used in the literature.[1-10] Although this model gives better predictions than those of the linear theory, it overestimates the frequency content or "broadening" of the response spectrum at high excitation levels.

To further improve the predictions of the nonlinear analysis, several damping models have been studied. Linear, nonlinear, and viscous damping are among the models used.[11-15] Prasad and Mei[16,17] used nonlinear damping in their large deflection model. A set of modal equations of the Duffing form coupled in the nonlinear stiffness and uncoupled in the nonlinear damping was derived. An approximate solution was obtained for rms quantities (such as displacement and strain) and spectral density functions by the equivalent linearization method. The nonlinear damping was found to contribute to the broadening of the power spectra at high excitation levels. However, Moyer[18] and Reinhall and Miles[19] showed that the method of equivalent linearization gives inaccurate response spectra for large deflections. The broadening of the response spectrum at high excitation levels was found to be caused by the nonlinear stiffness.[19] Robinson and Mei[20] studied the influence of nonlinear damping on panels' random response using a time domain simulation. They found that the nonlinear damping was responsible for a narrowing of the nonlinear response power spectrum.

Recently, Robinson et al.[21] used a finite element method to integrate the nonlinear plate equations with an equivalent linear viscous damping term to study the linear and nonlinear responses of a plate to a narrow-band random excitation. Their results were in good agreement with experiments for low excitation levels. However, for high excitation levels, the model overpredicted the broadening of the response spectrum and predicted higher response levels at high frequencies.

In most structural dynamics analyses, there is little discussion about the effect of the surrounding acoustic fluid on the response of a structure to a given excitation field. Frendi et al.[22,23] showed that a strong coupling between plate vibration and the surrounding flowfields exists at high excitation levels.

In this paper, an attempt is made to explain the discrepancies between the experimental and numerical results obtained by Robinson et al.[21] Using the model developed by Frendi et al.[23] and changing the configuration of the computational domain to match that of the experiments, the response of a flexible plate to both a narrow-band random excitation and a harmonic excitation is studied using two models. One model accounts for the full nonlinear coupling to the surrounding fluid. The other replaces the nonlinear coupling by an equivalent linear viscous damping on the plate.

The remainder of the paper is organized as follows. In Sec. II, a detailed description of the analytical model is given. Section III describes the numerical techniques, and the results are discussed in Sec. IV. Finally, the conclusions are given in Sec. V.

II. Formulation of the Model

As shown in Fig. 1, the computational domain is composed of three regions. The acoustic fluid in the cavity region (or top domain) is separated from that in the open space region (or bottom domain) by a flexible plate clamped between two rigid plates. Acoustic disturbances are introduced at the left boundary of the top domain and propagate over the rigid and flexible surfaces. There is no meanflow on either side of the flexible plate. The governing equations in the acoustic fluid

Received Jan. 11, 1993; revision received April 15, 1993; accepted for publication April 15, 1993.

*Research Scientist. Member AIAA.
†Aerospace Engineer, MS 463. Member AIAA.

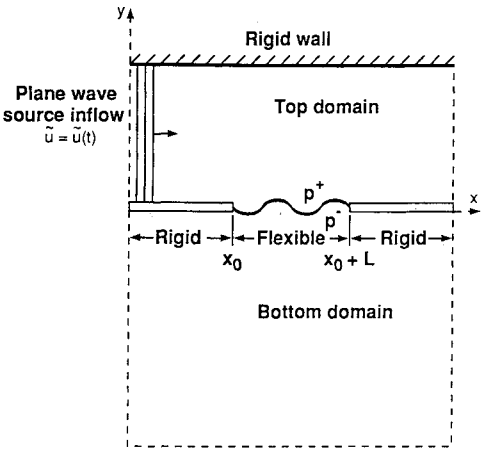

Fig. 1 Computational domain.

regions are the two-dimensional, compressible, nonlinear Euler equations. In a cartesian coordinate system, x and y, these equations can be written in conservation form as

$$\frac{\partial Q}{\partial t} = \frac{\partial F}{\partial x} + \frac{\partial G}{\partial y} \tag{1}$$

where Q is the vector $(\rho, \rho u, \rho v, e)^T$, ρ is the density, ρu and ρv are the x and y momenta, respectively, and e is the total energy per unit volume given by

$$e = \tfrac{1}{2}\rho(u^2 + v^2) + \rho c_v T \tag{2}$$

In Eq. (1), the functions F and G are

$$F = \begin{bmatrix} \rho u \\ \rho u^2 + p \\ \rho uv \\ u(e+p) \end{bmatrix}, \qquad G = \begin{bmatrix} \rho v \\ \rho uv \\ \rho v^2 + p \\ v(e+p) \end{bmatrix} \tag{3}$$

In addition to Eq. (1), an ideal gas state equation is used

$$p = \rho RT \tag{4}$$

where p is the pressure, R is the gas constant, and T is the temperature.

The motion of the plate is approximated by the one-dimensional equation given by

$$D\frac{\partial^4 w}{\partial x^4} - N_x\frac{\partial^2 w}{\partial x^2} + \rho_p h\frac{\partial^2 w}{\partial t^2} + (\Gamma_s + \Gamma_a)\frac{\partial w}{\partial t} = \Delta p \tag{5}$$

where w is the plate transverse deflection, ρ_p is the mass per unit volume of the plate, and h is the plate thickness. The total viscous damping is the sum of the structural damping Γ_s and the acoustic damping Γ_a. When the plate vibration is coupled to the surrounding acoustic fluid, $\Gamma_a = 0$. In Eq. (5), $D = Eh^3/12(1-\nu^2)$ is the stiffness of the plate, with E being the modulus of elasticity and ν the Poisson ratio of the plate material. The coefficient N_x in Eq. (5) is given by

$$N_x = \frac{Eh}{2L}\int_{x_0}^{x_0+L}\left(\frac{\partial w}{\partial x}\right)^2 dx \tag{6}$$

which represents the tension created by stretching of the plate due to bending. In Eq. (6) x_0 is the origin of the flexible plate and L its length. The forcing term on the right-hand side of Eq. (5) is

$$\Delta p = p^- - p^+ \tag{7}$$

where p^+ and p^- are the pressures on the surfaces above and below the plate, respectively. When acoustic coupling is neglected, the plate response is obtained by neglecting p^- in Eq. (5) and using the same p^+ at the plate center as that obtained by integration of the Euler equations. This is done to reproduce the results obtained by Robinson et al.[21]

Equations (1-7) are written in a nondimensional form using the following reference quantities for the different variables:

$$(x, y, w)_{\text{ref}} = l_{\text{ref}}, \qquad t_{\text{ref}} = \frac{l_{\text{ref}}}{c_\infty}, \qquad T_{\text{ref}} = \frac{c_\infty^2}{c_v}$$

$$\rho_{\text{ref}} = \rho_\infty, \qquad \left(u, v, \frac{\partial w}{\partial t}\right)_{\text{ref}} = c_\infty, \qquad (p, e)_{\text{ref}} = \rho_\infty c_\infty^2 \tag{8}$$

The notation $(\cdot, \cdot)_{\text{ref}}$ is used to represent the reference quantity of the variables in parentheses. The various freestream fluid properties are those of air at sea level conditions, which are temperature $T_\infty = 519°\text{R}$, density $\rho_\infty = 1.147 \times 10^{-7}$ lbf·s^2/in.^{4}, pressure $p_\infty = 14.7$ psi, and sound speed $c_\infty = 13392$ in./s. The specific heat at constant volume is $c_v = 6.1776 \times 10^5$ in.^{2}/(s^2 °R), the ratio of specific heats is $\gamma = c_p/c_v = 1.4$, and the reference length is $l_{\text{ref}} = 12.0$ in.

III. Method of Solution

The unsteady Euler equations [Eq. (1)] are solved using an explicit finite difference scheme. The scheme, which is a generalization of MacCormack's scheme obtained by Gottlieb and Turkel,[24] is fourth-order accurate in space and second-order accurate in time. The numerical scheme, applied to a one-dimensional equation of the form

$$\frac{\partial u}{\partial t} = \frac{\partial F}{\partial x} \tag{9}$$

consists of a predictor step given by

$$u_i^* = u_i^n + \frac{\Delta t}{6\Delta x}(-7F_i + 8F_{i+1} - F_{i+2}) \tag{10}$$

followed by a corrector step of the form

$$u_i^{n+1} = \tfrac{1}{2}\left[u_i^* + u_i^n + \frac{\Delta t}{6\Delta x}(7F_i^* - 8F_{i-1}^* + F_{i-2}^*)\right] \tag{11}$$

In those equations, the subscript i denotes the spatial grid point and the superscript n the time level. The fourth-order accuracy is obtained by alternating the previous scheme with its symmetric variant.[24] Operator splitting is used to reduce the two-dimensional problem to a sequence of one-dimensional problems. If L_x and L_y denote the solution operators for the one-dimensional x and y problems, then the solution to Eq. (1) is obtained by

$$Q^{n+2} = L_x L_y L_y L_x Q^n \tag{12}$$

Further details regarding the method and the advantage of fourth-order schemes can be found in Bayliss et al.[25]

The boundary conditions employed on the rigid and flexible surfaces for the Euler equations are

$$v = 0 \qquad T = T_w \tag{13}$$

over the rigid surfaces, and

$$v = \frac{\partial w}{\partial t} \qquad T = T_w \tag{14}$$

over the flexible surface. In Eqs. (13) and (14) T_w is a specified wall temperature; in this paper it is taken to be the freestream temperature T_∞. The x-component of the velocity (u) is obtained through linear extrapolation from the interior of the computational domain over both the rigid and flexible surfaces.

The pressure boundary conditions are as follows: over the rigid surfaces where the time rate of change of the normal momentum is zero, the pressure is calculated using the normal momentum equation by simply imposing the normal gradient of the sum of pressure and vertical momentum flux to be zero $[\partial/\partial y(p + \rho v^2) = 0]$. Over the flexible part of the surface, a linear extrapolation from the interior of the computational domain is used. At the left boundary of the top domain, a nondimensional perturbation velocity is specified $\tilde{u}$ as

$$\tilde{u} = \epsilon R(t) \qquad \text{or} \qquad \tilde{u} = \epsilon \sin(\omega t) \tag{15}$$

where $R(t)$ represents a narrow-band random excitation, and $\tilde{u}$ is a nondimensional perturbation velocity. In Eq. (15), ϵ is the peak amplitude of the disturbance for the harmonic case (with ω being the frequency), and is an rms amplitude in the random case. Using the routine RNNOF of the IMSL library,[26] Gaussian random data is generated; then, using a quadratic narrow-band filter, the data is filtered to give the desired input. The pressure and vertical velocity (v) are obtained by linear extrapolation from the interior of the computational domain, and the temperature is imposed to be constant ($T = T_w$). The remaining nonphysical boundary conditions (top domain right boundary, bottom domain right, left, and bottom boundaries) are derived using the method of characteristics.[27,28]

The plate equation is integrated using an implicit finite difference method for structural dynamics developed by Hoff and Pahl.[29] The calculation of N_x was done using Simpson's rule of integration. The boundary conditions used to solve the plate equation are those for a clamped plate

$$w = \frac{\partial w}{\partial x} = 0 \qquad \text{at} \qquad x = x_0,\ x_0 + L \tag{16}$$

The coupling between the acoustic fluid and the flexible plate is performed as follows. The method used in the fluid is explicit. Thus the pressure fields in the top and bottom domains are updated by using the value of $\partial w/\partial t$ at the previous time step as a boundary condition for the Euler equations. Then, using the new values of p^+ and p^-, the plate equation is integrated to obtain the new vertical velocity $\partial w/\partial t$. This procedure is repeated at every time step.

For every coupled calculation, the time history of the pressure at the center of the flexible plate in the top domain is stored to be used as input for the equivalent uncoupled case. This procedure was done to match the numerical used by Robinson et al.[21]

The use of Eq. (5) to approximate the motion of the plate is justified by Eqs. (15) and (16), which indicate that the load is uniform in the spanwise direction [Eq. (15)] and that the plate is clamped only in the streamwise direction (x-direction) [Eq. (16)]. Therefore, the motion of the plate is dominated by the streamwise modes.

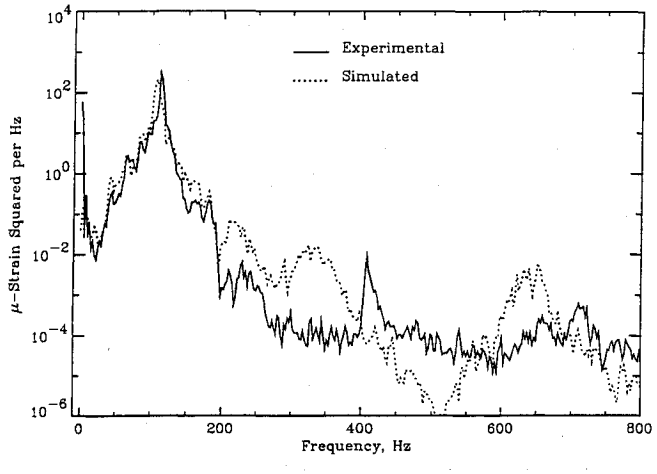

Fig. 2 Experimental and simulated power spectra of the strain for an overall sound pressure level of 140 dB (Ref. 21).

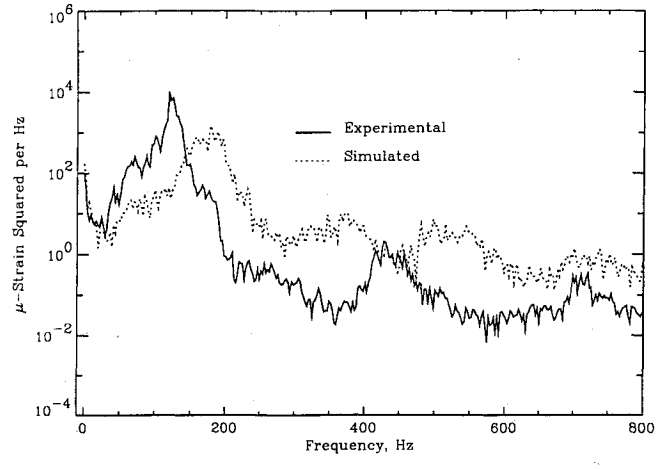

Fig. 3 Experimental and simulated power spectra of the strain for an overall sound pressure level of 160 dB (Ref. 21).

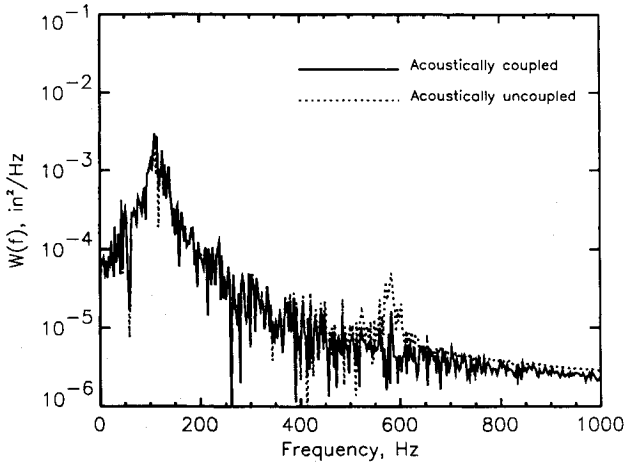

Fig. 4 Comparison of the power spectra of the center plate displacement obtained by the coupled and uncoupled models for a maximum random excitation level of 120 dB.

IV. Results and Discussion

The results presented in this paper are obtained for a flexible plate having the following properties: stiffness $D = 1095.6$ lbf · in., mass per unit area $\rho_p h = 2.21 \times 10^{-5}$ lbf · s^2/in.^{3}, and a Poisson ratio $\nu = 0.3$. Two values of total viscous damping ($\Gamma_s + \Gamma_a$) are used: 2.5×10^{-5} lbf · s/in.^{3} used in the fully coupled calculation (where $\Gamma_a = 0$) and 5×10^{-4} lbf · s/in.^{3} used in the uncoupled calculation. These two values are chosen such that the two calculations predict the same response for low-intensity excitations (linear vibration regime). The plate is 15 in. long, 11 in. wide, and 0.13 in. thick. The first natural frequency of the plate is 112 Hz. The top domain of Fig. 1 is 12 in. high in the y-direction and 120 in. long in the x-direction, and the number of computational points used are 101 and 181 in each direction, respectively. The bottom domain is 120 in. long in both directions with 161 points used in each direction.

The power spectra shown here are for the center plate displacement response and the pressure on either side of the plate center. Also, typical instantaneous pressure distributions are shown for both the top and bottom domains.

A. Previous Experimental and Numerical Results

At first the results obtained in Ref. 21 are summarized. Figure 2 shows the power spectral density of the strain ob-

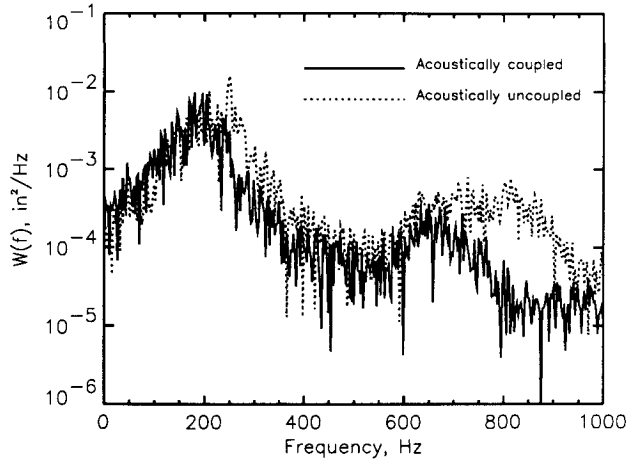

Fig. 5 Comparison of the power spectra of the center plate displacement obtained by the coupled and uncoupled models for a maximum random excitation level of 140 dB.

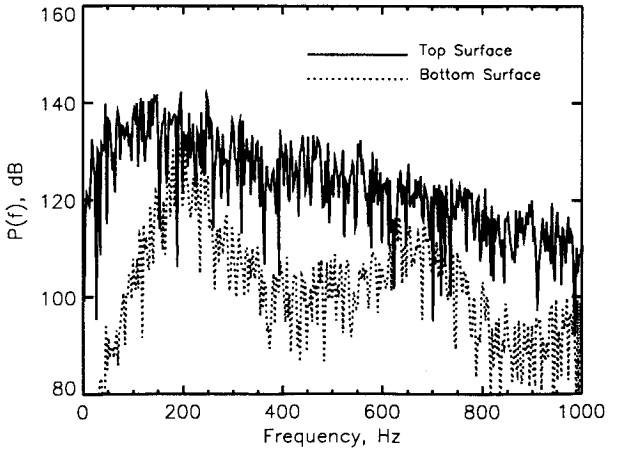

Fig. 6 Power spectra of the surface pressure on both sides of the plate center.

tained both experimentally and numerically for a narrow-band excitation sound pressure level of 140 dB. The figure shows that the power spectrum obtained from the simulation is in good agreement with that given by the experiment near the fundamental frequency (112 Hz), where the measured strains are within the sensitive range of the strain gages. Away from the fundamental frequency, the measured strains are small compared with the sensitivity, which is approximately 1.0 μ-strain squared per Hz, and therefore not very accurate. As the sound pressure level is increased to 160 dB, Fig. 3, the simulation overpredicts the broadening of the spectrum and the response at high frequencies. It is important to restate that an equivalent linear viscous damping was used in the plate model, and that the nonlinear coupling to the surrounding acoustic fluid was neglected.

B. Current Model

1. Random Excitation

To obtain a pressure input spectrum similar to that of the experiments described earlier, the random data generated by the IMSL routine RNNOF is filtered using a quadratic narrow-band filter of bandwidth 50 to 500 Hz. Figure 4 shows that both the fully coupled and uncoupled models predict the same displacement frequency response of the plate for a low-intensity noise having a maximum sound pressure level of 120 dB. The spectrum obtained by the uncoupled model shows a more pronounced peak at 560 Hz, which corresponds to a natural frequency of the plate. The plate response is linear and is dominated by the first mode. Because of the high cost in CPU time of the coupled calculations, the time histories of the various quantities were not long enough to give smoother power spectra.

Increasing the noise intensity to a maximum sound pressure level of 140 dB leads to a nonlinear plate response. The frequency content of the response shifts toward higher frequencies and the spectrum broadens, as shown by Fig. 5. However, the shift and the broadening are different for the two models. The power spectrum predicted by the uncoupled model shows a greater shift toward high frequencies and more broadening than that predicted by the coupled model. The plate response at high frequencies is also higher when the uncoupled model is used. The difference between the coupled and uncoupled power spectra is similar to that observed earlier between experiments and simulation (see Fig. 3). This result indicates that acoustic coupling at high sound pressure levels is important for the accurate prediction of the plate response.

Figure 6 shows the power spectra of the pressure on both sides of the plate center. Notice that the pressure on the top surface is dominated by the input pressure, whereas the pressure on the bottom surface is due to the vibration of the plate and has, therefore, a power spectrum similar to that of the response. An instantaneous pressure distribution in the top domain is shown in Fig. 7. Because the input is random, several peaks are observed in the pressure field superimposed on a strong low frequency. The instantaneous pressure distribution in the bottom domain shows the presence of one dominant frequency corresponding to that of the plate response (see Fig. 8).

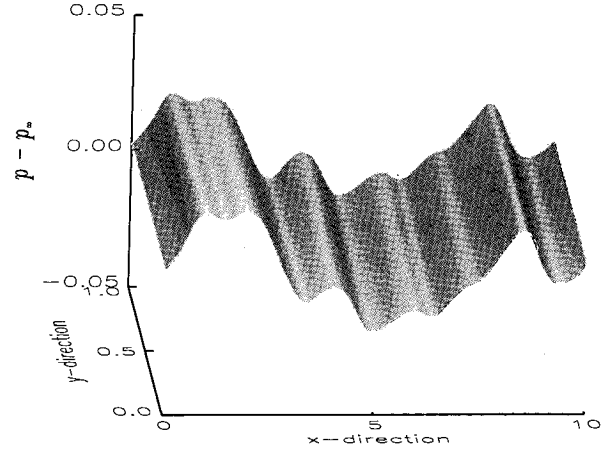

Fig. 7 Instantaneous pressure distribution in the top domain for a maximum random excitation of 140 dB.

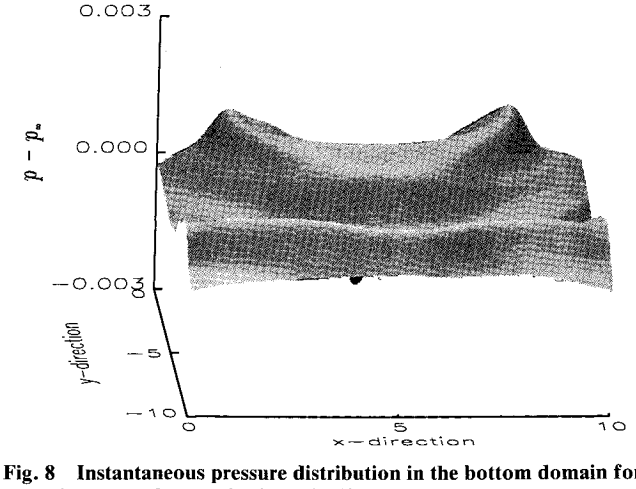

Fig. 8 Instantaneous pressure distribution in the bottom domain for a maximum random excitation of 140 dB.

2. Harmonic Excitation

For an excitation frequency $f = 112$ Hz (corresponding to the first mode of the plate) and an amplitude of 150 dB, the plate response is nonlinear, as shown by Fig. 9. The power spectra of the center plate displacement show several harmonics and subharmonics characteristic of the nonlinear response. For this excitation level, both the fully coupled and uncoupled models predict the same response power spectrum. (Similar results are obtained for lower dB levels.) This result is attributed to the weak nonlinearity in the radiation field. Figure 10 shows the power spectra of the pressure on both sides of the plate center. The power spectrum of the pressure on the top

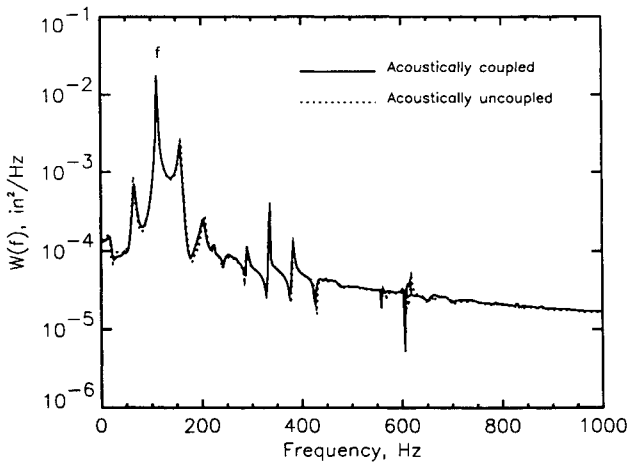

Fig. 9 Comparison of the power spectra of the center plate displacement obtained by the coupled and uncoupled models for harmonic excitation with a frequency of 112 Hz and a peak amplitude of 150 dB.

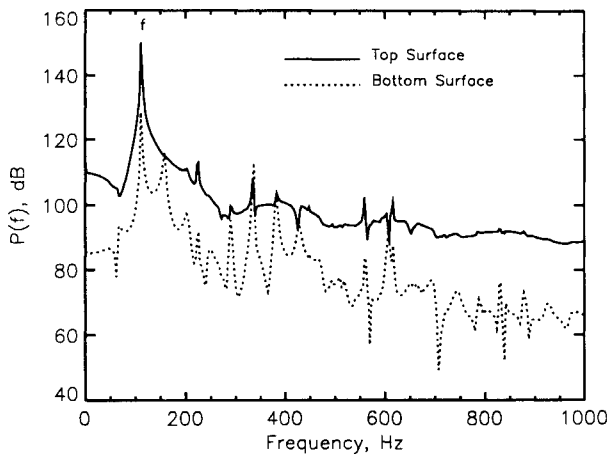

Fig. 10 Power spectra of the surface pressure on both sides of the plate center.

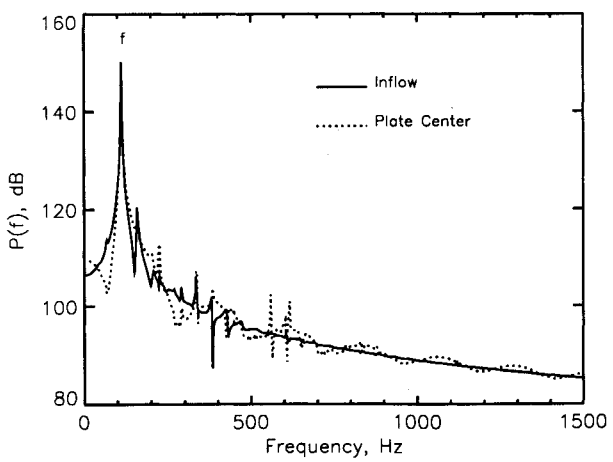

Fig. 11 Power spectra of the top domain pressures at the inflow and near the center of the flexible plate.

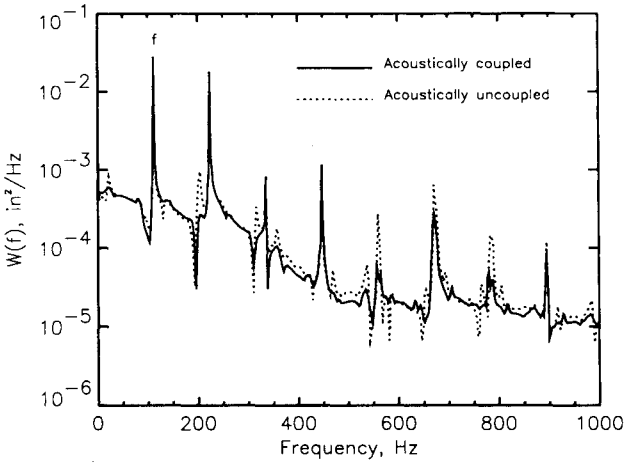

Fig. 12 Comparison of the power spectra of the center plate displacement obtained by the coupled and uncoupled models for harmonic excitation with a frequency of 112 Hz and a peak amplitude of 165 dB.

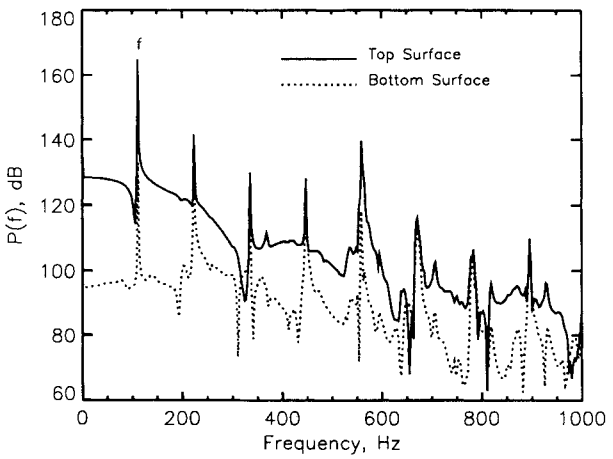

Fig. 13 Power spectra of the surface pressure on both sides of the plate center.

surface shows a strong peak at the fundamental frequency (112 Hz) and negligible harmonic content, indicative of weak nonlinearity. The power spectrum of the radiated pressure on the bottom surface is similar to the response power spectrum with slightly stronger harmonics as should be expected, because the coupling between the plate vibration and the acoustic fluid is obtained through the vertical velocity. Due to transmission loss, the level of the radiated pressure on the bottom surface is 20 dB lower than that on the top surface. The weak nonlinearity in the pressure field is further evidenced by Fig. 11, where the top domain power spectra of the pressures at the inflow and near the center of the flexible plate are shown. The two spectra are nearly identical except for a negligible difference in the levels of the harmonics indicating a weak nonlinearity in addition to the contribution of the flexible plate.

Increasing the level of the excitation source to 165 dB leads to a stronger contribution of the harmonics to the plate response and much less contribution from the subharmonics (see Fig. 12). This result is in agreement with earlier work,[23] which showed that the window to complex dynamics is very narrow and that an increase in excitation level can lead to a more stable system. The two models do not predict the same displacement power spectrum of the plate. At high frequencies, the uncoupled model predicts a higher level of the response peaks. This prediction is similar to the random excitation case, except that the peaks are not shifted. Figure 13 shows that the pressure fields on both sides of the plate are nonlinear. Both pressure power spectra show a strong harmonic content. The nonlinearity in the top domain pressure field is shown in Fig. 14. The levels of the harmonics on the flexible plate are

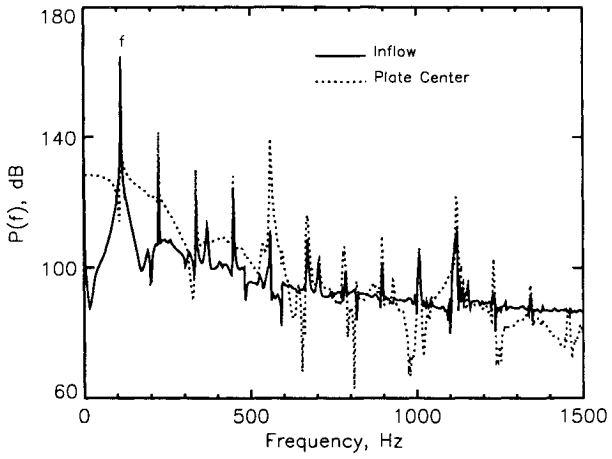

Fig. 14 Power spectra of the top domain pressures at the inflow and near the center of the flexible plate.

higher due to both the plate vibrations and the nonlinear wave propagation. The latter point can be seen on the figure through the change in magnitude of the peak at 560 Hz and its harmonic 1120 Hz. On the flexible plate, the 560 Hz peak (which corresponds to a plate mode) is higher than its harmonic (1120 Hz). However, at the inflow the two peaks are nearly the same. This result indicates that although the 560 Hz peak has decayed significantly, its harmonic has decayed only slightly. This behavior is a characteristic of nonlinear wave propagation. Similar results are obtained for the bottom domain pressure field.

V. Conclusions

Based on the results obtained in this paper, the following conclusions can be made:

1) The coupling between the acoustic fluid with no mean-flow and the plate vibration is not important at low excitation levels for both random and harmonic excitations, as was reported by Frendi et al.[23]

2) The acoustic coupling is important for accurate prediction of the plate response at high excitation levels. The present results show that the absence of acoustic coupling in earlier models may be one of the reasons for the discrepancy between numerical and experimental results. When acoustic coupling is accounted for, less spectral broadening and frequency shift is obtained. The plate response is lower at higher frequencies, a result that is in agreement with experimental observations.[21]

3) In the harmonic case, no shift in the peaks of the response is obtained; however, the uncoupled model predicts higher levels of the higher harmonics. The results also show that the coupling between the acoustic fluid and the plate vibration is important only when both the structural response and the acoustic radiation are nonlinear, a result that is in agreement with previous results.[23]

Acknowledgment

The first author was supported by NASA Langley Research Center under Contract NAS1-19317.

References

[1]Tseng, W. Y., and Dugundji, J., "Nonlinear Vibrations of a Beam Under Harmonic Excitation," *Journal of Applied Mechanics,* Vol. 37, No. 2, 1970, pp. 292-297.

[2]Srinivasan, A. V., "Non-linear Vibrations of Beams and Plates," *International Journal of Non-linear Mechanics,* Vol. 1, No. 4, 1966, pp. 179-191.

[3]Maestrello, L., Frendi, A., and Brown, D. E., "Nonlinear Vibration and Radiation From a Panel with Transition to Chaos Induced by Acoustic Waves," *AIAA Journal,* Vol. 30, No. 11, 1992, pp. 2632-2638.

[4]Yamaki, N., and Mori, A., "Nonlinear Vibrations of a Clamped Beam with Initial Deflection and Initial Axial Displacement, Part I: Theory," *Journal of Sound and Vibration,* Vol. 71, No. 3, 1980, pp. 333-346.

[5]Yamaki, N., Otomo, K., and Mori, A., "Nonlinear Vibrations of a Clamped Beam with Initial Deflection and Initial Axial Displacement, Part II: Experiment," *Journal of Sound and Vibration,* Vol. 71, No. 3, 1980, pp. 347-360.

[6]Ibrahim, R. A., and Roberts, J. W., "Broad-Band Random Excitation of a Two Degree-of-Freedom System with Autoparametric Coupling," *Journal of Sound and Vibration,* Vol. 44, No. 3, 1976, pp. 335-348.

[7]Mei, C., and Decha-Umphai, K., "A Finite Element Method for Nonlinear Forced Vibrations of Beams," *Journal of Sound and Vibration,* Vol. 102, No. 3, 1985, pp. 369-380.

[8]Chia, C. Y., *Nonlinear Analysis of Plates,* McGraw-Hill, New York, 1980, pp. 1-51.

[9]Dowell, E. H., "Flutter of a Buckled Plate as an Example of Chaotic Motion of a Deterministic Autonomous System," *Journal of Sound and Vibration,* Vol. 85, No. 3, 1982, pp. 333-344.

[10]Dowell, E. H., and Pezeshki, C., "On the Understanding of Chaos in Duffings Equation Including a Comparison with Experiment," *Journal of Applied Mechanics,* Vol. 53, No. 1, 1986, pp. 5-9.

[11]Reed, R. R., "Analysis of Structural Response with Different Forms of Damping," NASA TND-3861, July 1967.

[12]Jacobsen, L. S., "Steady State Vibration as Influenced by Damping, Part I," *Transactions of the American Society of Mechanical Engineers,* Vol. 52, No. 1, 1930, pp. 169-181.

[13]Torres, M. R., and Mote, C. D., Jr., "Expected Equivalent Damping Under Random Excitation," *Journal of Engineering for Industry, Transactions of the American Society of Mechanical Engineers,* Vol. 91, No. 4, 1969, pp. 967-974.

[14]Tang, D. M., and Dowell, E. H., "Random Response of Beams and Plates with Slipping at the Support Boundaries," AIAA Paper 86-0931, May 1986.

[15]Dowell, E. H., "Damping in Beams and Plates Due to Slipping at the Support Boundaries," *Journal of Sound and Vibration,* Vol. 105, No. 2, 1986, pp. 243-253.

[16]Mei, C., and Prasad, C. B., "Effects of Non-linear Damping on Random Response of Beams to Acoustic Loading," *Journal of Sound and Vibration,* Vol. 117, No. 1, 1987, pp. 173-186.

[17]Prasad, C. B., "The Effects of Nonlinear Damping on the Large Deflection Response of Structures Subjected to Random Excitation," Ph.D. Dissertation, Mechanical Engineering Dept., Old Dominion Univ., Norfolk, VA, 1987.

[18]Moyer, E. T., Jr., "Time Domain Simulation of the Response of Geometrically Nonlinear Panels Subjected to Random Loading," *Proceedings of the AIAA/ASME/ASCE/AHS 29th Structures, Structural Dynamics, and Materials Conference* (Williamsburg, VA), AIAA, Washington, DC, April 1988, pp. 210-218.

[19]Reinhall, P. G., and Miles, R. N., "Effect of Damping and Stiffness on the Random Vibration of Non-Linear Periodic Plates," *Journal of Sound and Vibration,* Vol. 131, No. 1, 1989, pp. 33-42.

[20]Robinson, J., and Mei, C., "The Influence of Nonlinear Damping on the Random Response of Panels by Time Domain Simulation," AIAA Paper 89-1104, April 1989.

[21]Robinson, J., Rizzi, S., Clevenson, S., and Daniels, E., "Large Deflection Random Response of Flat and Blade Stiffened Carbon-Carbon Panels," AIAA Paper 92-2390, May 1992.

[22]Frendi, A., Maestrello, L., and Bayliss, A., "On the Coupling Between a Supersonic Laminar Boundary Layer and a Flexible Surface," Inst. for Computer Application in Science and Engineering, Rept. 92-42, Hampton, VA, Sept. 1992.

[23]Frendi, A., Maestrello, L., and Bayliss, A., "Coupling Between Plate Vibration and Acoustic Radiation," AIAA Paper 93-0606, Jan. 1993.

[24]Gottlieb, D., and Turkel, E., "Dissipative Two-Four Methods for Time Dependent Problems," *Mathematics of Computation,* Vol. 30, No. 136, 1976, pp. 703-723.

[25]Bayliss, A., Parikh, P., Maestrello, L., and Turkel, E., "A Fourth Order Scheme for the Unsteady Compressible Navier-Stokes Equations," AIAA Paper 85-1694, July 1985.

[26]International Mathematical and Statistical Library, Version 2.0, Vol. 3, Houston, TX, 1991, p. 1317.

[27]Abarbanel, S. S., Don, W. S., Gottlieb, D., Rudy, D. H., and Townsend, J. C., "Secondary Frequencies in the Wake of a Circular Cylinder with Vortex Shedding," Inst. for Computer Application in Science and Engineering, Rept. 90-16, Hampton, VA, July 1990.

[28]Givoli, D., "Non-reflecting Boundary Conditions," *Journal of Computational Physics,* Vol. 94, No. 1, 1991, pp. 1-29.

[29]Hoff, C., and Pahl, P. J., "Development of an Implicit Method With Numerical Dissipation From a Generalized Single-Step Algorithm for Structural Dynamics," *Computational Methods in Applied Mechanical Engineering,* Vol. 67, No. 2, 1988, pp. 367-385.